First-principles study of Mn-induced local magnetic moments in host semiconductors

Shi-Hao Wei
Physics Department, Fudan University, Shanghai-200433, China

X. G. Gong
Physics Department, Fudan University, Shanghai 200433, China
and Institute of Solid State Physics, Chinese Academy of Sciences, Hefei 230031, China

Gustavo M. Dalpian and Su-Huai Wei
National Renewable Energy Laboratory, Golden, Colorado 80401, USA
(Received 5 January 2005; published 15 April 2005)

Using the first-principles method, we calculate the atom and angular momentum resolved local moments in diluted GaMnAs, GaMnN, and CdMnTe. We show that the local moments are correlated with magnetic stability and can be explained by the occupation and hybridization of the host states with the Mn 3*d* states in both spin channels. We also show that the splitting of the localized core orbitals follow the sign of the local magnetic moments, but for the delocalized valence states the splitting is determined by hybridization with Mn states. We propose that spin-polarized photoemission measurement of the shallow core states could be used to measure the local moments of the host elements.

DOI: 10.1103/PhysRevB.71.144409 PACS number(s): 75.50.Pp, 71.55.Eq, 71.70.−d

I. INTRODUCTION

Because of the coupling of host *s* and *p* states with localized Mn 3*d* states, Mn-doped II-VI and III-V diluted magnetic semiconductors (DMS) exhibit interesting properties that combine semiconductor electronics with magnetism.[1–4] Most of the Mn DMS, such as CdMnTe, shows antiferromagnetic behavior caused by the superexchange interaction, where occupied Mn *d* states couple with the neighboring unoccupied Mn *d* states, thus lowering the total energy.[1,5] However, recent discovery that Mn-doped III-V semiconductors can have ferromagnetic ground states[2] has led to an intensified search for high-T_c ferromagnetic DMS and stimulated investigations to understand the mechanism of ferromagnetic exchange in these systems.

It is now well established that the presence of holes is crucial for the ferromagnetism in Mn doped III-V systems.[3,6–9] This can be understood through band-structure models. As an example, we show schematically in Fig. 1 where the hole is at the valence band edge (e.g., GaMnAs). In the ferromagnetic case, the exchange splitting caused by coupling between host *p* state and Mn (occupied and unoccupied) *d* state pushes one spin state upward and the opposite spin state downward relative to the antiferromagnetic case. When the hole is present, it occupies the high energy state, thus lowering the total energy. In the case where no hole is present, such as in CdMnTe, the ferromagnetic splitting does not lower the total energy to the first order, and thus the material remains antiferromagnetic through the superexchange. When the hole is at the Mn *d* level (e.g., GaMnN), the exchange splitting due mostly to the direct *d*-*d* coupling between the Mn ions is responsible for the ferromagnetic order.

It has been shown[10,11] that understanding the Mn ion-induced local magnetic moments in semiconductor host is a key issue in testing the various mechanism of ferromagnetic order in semiconductors. Recently, Keavney *et al.*,[11] using x-ray magnetic circular dichroism (XMCD), which measures the magnetic field-induced differential absorption of the $L_{3,2}$ edges of right and left circularly polarized x-ray radiation, have deduced for the first time the atom-resolved spin configuration in ferromagnetic diluted GaMnAs. They find that, in GaMnAs, the As local moment is antiparallel to the Mn, whereas Ga has a small parallel moment. However, their measurement is based on several assumptions whose validity is yet to be established. For example, they assumed the As valence 4*s* and 4*p* moments have the same sign as the exchange splitting and the XMCD spectrum follows the sign of the corresponding local moment.[12]

In this paper, using first-principles density functional theory, we calculate the band structures, density of states (DOS), and atom and angular momentum resolved local moments in diluted GaMnAs, GaMnN, and CdMnTe, as well as the hypothetical zinc-blende MnAs, MnN, and MnTe. We find that (i) in GaMnAs, the As local moment is antiparallel to the Mn. (ii) In CdMnTe, the Te local moment is parallel to the Mn. (iii) In GaMnN, depending on the Mn concentration, the sign of the N local moment could be either positive or negative. We show that these trends of local moments can be explained by the occupation and hybridization of the host states with the Mn 3*d* states in both spin channels and are consistent with available theoretical models of magnetic coupling in these systems.[3,6,7,9] We also find that (iv) the splitting of the core orbitals follow the sign of the local magnetic moments due to the direct (potential) exchange, but for *de-*

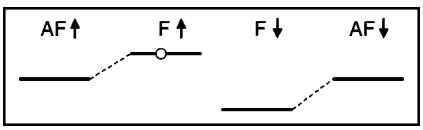

FIG. 1. Schematic model of hole-stabilized ferromagnetism.

TABLE I. Calculated lattice constants and the s, p, d, and total local moments (in μ_B) inside the MT spheres of zinc-blende ferromagnetic $Ga_{1-x}Mn_xAs$, $Ga_{1-x}Mn_xN$, and $Cd_{1-x}Mn_xTe$. Only the moments of the Mn atom and its nearest neighbor anion and cation atoms are shown.

Compounds	Atom	μ^{total}	μ^s	μ^p	μ^d	a (Å)
MnAs	Mn	3.57	0.05	0.03	3.49	5.700
	As	−0.16	0.01	−0.19	0.02	
Ga_3MnAs_4	Mn	3.57	0.04	0.03	3.50	
	As	−0.04	0.00	−0.05	0.01	5.752
	Ga	0.03	0.02	0.01	0.00	
$Ga_{15}MnAs_{16}$	Mn	3.62	0.04	0.04	3.54	
	As	−0.04	0.00	−0.05	0.01	5.765
	Ga	0.01	0.01	0.00	0.00	
MnN	Mn	1.39	0.02	0.00	1.37	4.378
	N	−0.04	0.00	−0.04	0.00	
Ga_3MnN_4	Mn	3.39	0.03	0.05	3.31	
	N	0.01	0.01	0.00	0.00	4.489
	Ga	0.05	0.02	0.02	0.01	
$Ga_{15}MnN_{16}$	Mn	3.37	0.02	0.05	3.30	
	N	0.01	0.01	0.00	0.00	4.512
	Ga	0.01	0.01	0.01	0.00	
MnTe	Mn	4.24	0.05	0.05	4.14	6.402
	Te	0.08	0.01	0.06	0.01	
Cd_3MnTe_4	Mn	4.12	0.04	0.03	4.05	
	Te	0.02	0.00	0.02	0.00	6.574
	Cd	0.02	0.01	0.01	0.00	
$Cd_{15}MnTe_{16}$	Mn	4.12	0.04	0.04	4.04	
	Te	0.01	0.00	0.01	0.00	6.617
	Cd	0.00	0.00	0.00	0.00	

localized host valence states, the splitting depends on the hybridization of these states with localized Mn 3*d* states, i.e., the kinetic exchange effect is more important. This indicates that the differential spin density of states (SDOS) of the delocalized valence states usually does not follow the sign of its local moment; thus deducing the local moment through the measurement of XMCD may require prior knowledge of the band structure.[11] We propose that direct spin-polarized photoemission measurement of the shallow core state could be a possible alternative to measure the local moments of host elements.

II. METHODS OF CALCULATION

The total energy and band structure calculations in this study were performed using the general potential linearized augmented plane wave (LAPW) method[13] within the local spin density approximation. For the exchange-correlation potential, we used the generalized gradient approximation (GGA) of Perdew and Wang.[14] The muffin-tin (MT) radii are 1.25 Bohr for N and 2.20 Bohr for all other elements. The local moments are defined as the moments within the MT spheres. Although this somewhat underestimates the true moments, especially for extended states, our test shows that the sign of the moment is independent of MT size. The Brillouin-zone integrations were performed using 60 Monkhorst-Pack special k-points[15] in the irreducible Brillouin zone of the zinc-blende phase and equivalent k-points for the superstructures. We find that GGA overestimates the lattice constants of GaAs and CdTe by less than 2%, but have much better agreement with experiment[16] for GaN and MnX (X=N, As, and Te) in their respective ground states.[17] For the alloys, we assume Vegard's rule is obeyed, but the internal atomic positions are fully relaxed.

III. RESULTS AND DISCUSSION

The calculated lattice constants and local moments of $Ga_{1-x}Mn_xAs$, $Ga_{1-x}Mn_xN$, and $Cd_{1-x}Mn_xTe$ are shown in Table I. For each system, we calculated the results at $x=1.0$, $x=0.25$, and $x=0.0625$, respectively. There are one Mn per unit cell. Figure 2 shows the calculated band structures at $x=1.0$ and $x=0.25$, and Fig. 3 shows the spin-density contour of the three systems. For GaMnAs, we find the local magnetic moment of Mn is close to 3.6 μ_B, whereas for the nearest neighbor As atom, the moment is negative (i.e., antiparallel to the Mn moment). This can also be observed in Fig. 3(a). The magnitude of the As moment at dilute limit

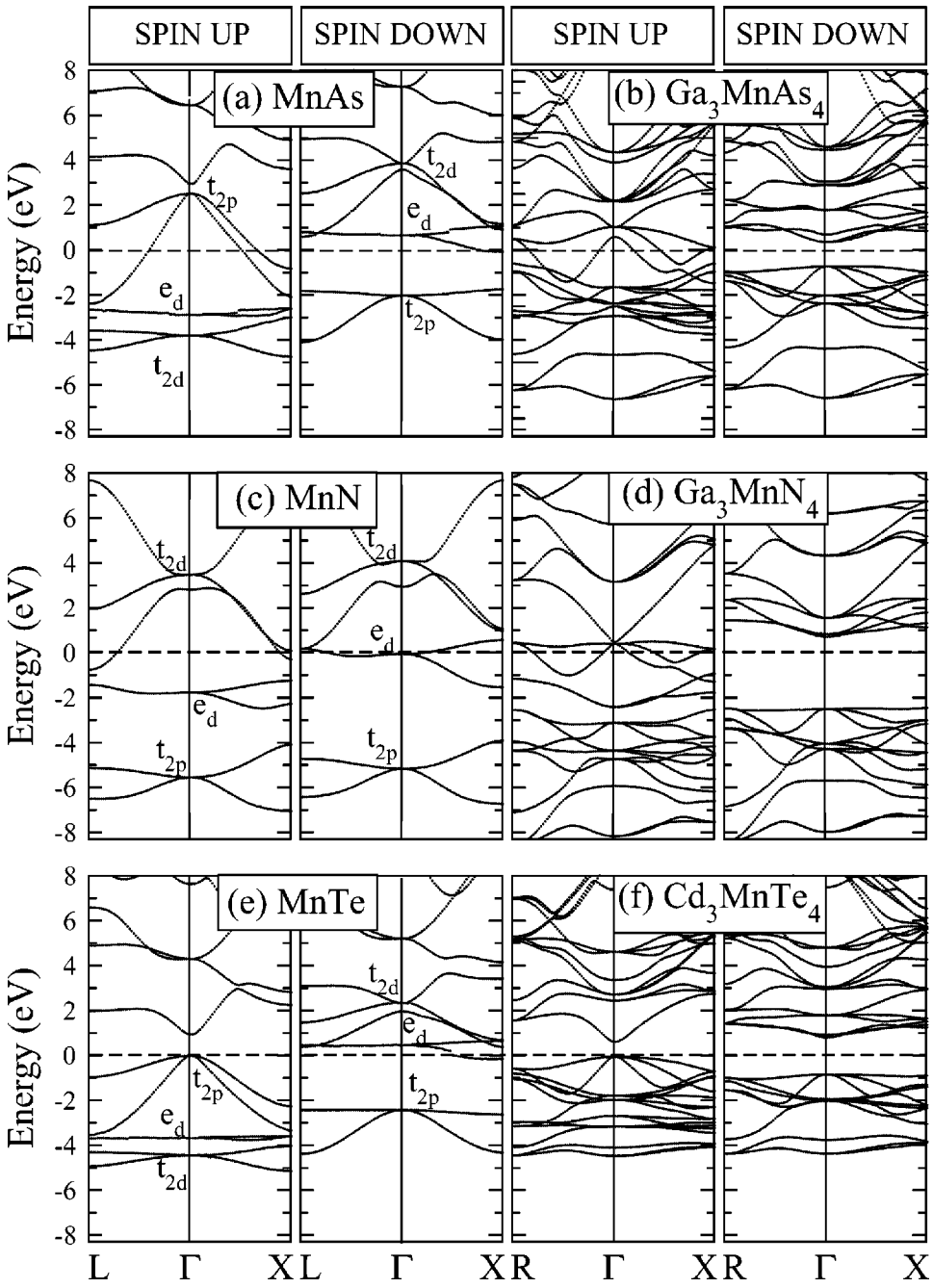

FIG. 2. Calculated band structures for the three systems. The dashed line shows the Fermi energy. The labels indicate the majority character of the bands at the Γ point.

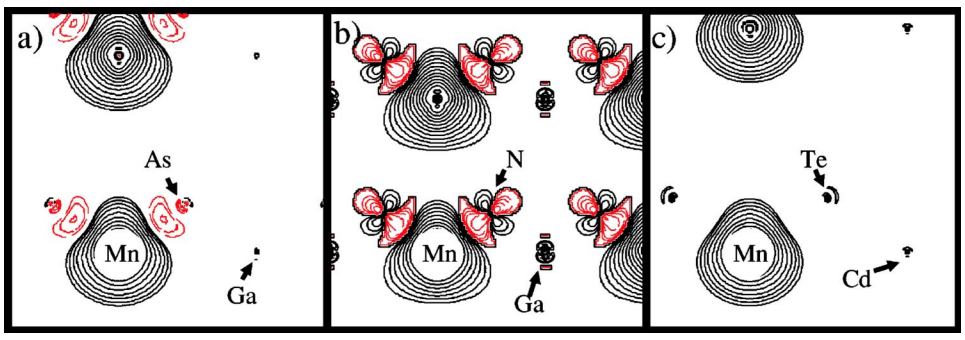

FIG. 3. (Color online) Contour plot of the spin density for (a) $Ga_{1-x}Mn_xAs$, (b) $Ga_{1-x}Mn_xN$, and (c) $Cd_{1-x}Mn_xTe$ at $x=0.25$. Solid black lines represent positive charge densities and dashed red lines indicate negative charge density. The charges are in the logarithmic scale.

($-0.04\ \mu_B$) is about four times smaller than that at $x=1$ ($-0.16\ \mu_B$). This is consistent with the fact that at dilute limit As has only one Mn nearest neighbor, whereas at $x=1$, As has four Mn neighbors. The Ga atom has a slightly positive moment. The moments decay very fast when it is further away from the Mn atom. Our results are consistent with previous calculations[18,19] and the results deduced from the XMCD measurements.[11]

To understand the results, we note that the local magnetic moment of an element is determined by two factors: (i) the occupation of the corresponding spin-up and spin-down bands and (ii) the hybridization of the states with other *occupied and unoccupied* states. For example, for the Mn atom in GaAs, Hund's rule for the half-filled 3*d* shell is obeyed. The five spin-up 3*d* states are occupied, whereas the five spin-down 3*d* states are unoccupied [Fig. 2(a)], thus the local magnetic moment of Mn would be close to 5 μ_B if the Mn does not couple to host elements. However, because the Mn t_{2d} state has the same symmetry as the anion t_{2p} state in the crystal, the two states couple strongly with each other (Fig. 2).[5] This coupling has two important effects. (a) It pushes the spin-up t_{2p} level upward and the spin-down t_{2p} level downward, resulting in a negative exchange splitting of the anion *p* state.[20] The hole introduced by the Mn substitution on the Ga site is located in the spin-up channel. (b) The coupling leads to wave function hybridization, which introduces a Mn *d* character into the nominally anion t_{2p} state and an anion *p* character into nominally Mn t_{2d} states (see Fig. 4). Because this hybridization introduces the spin-down Mn 3*d* character into the occupied states and, furthermore, the hole is on the spin-up t_{2p} state with spin-up Mn 3*d* character, the local moment at the Mn site is significantly reduced. This explains why the Mn local moment (3.6 μ_B) in GaMnAs is much smaller than the 5 μ_B one may expect from the simple Hund's rule.[18,21] Moreover, because the hole is on the spin-up t_{2p} state, it also explains why As has a negative local moment with mostly As 4*p* character. It is interesting to note in Table I that the As *s* orbital moment is *positive*, i.e., opposite to the As *p* moment. This is because the hole at valence band maximum (VBM) has mostly As *p* characters,[5] and the As *s* and Mn *d* coupling is not allowed by symmetry at the zone center.

The situation in the CdMnTe system is different from that in GaMnAs, because the substitution of Mn on the Cd site does not introduce holes.[1,5] This has the following consequences. (a) The filling of the spin-up hole state increases the local moment of Mn in CdMnTe relative to that in GaMnAs, because the hybridized hole state contains spin-up Mn 3*d* character. (b) The filled spin-up hole state contains mostly anion *p* orbital. Furthermore, because the hybridization between the spin-down Te t_{2p} state and the unoccupied spin-down Mn t_{2d} state reduces the spin-down Te 5*p* content (see Fig. 4), it also explains why the Mn-induced local moment of Te in CdMnTe is positive [i.e., parallel to the Mn moment, see also Fig. 3(c)].

For GaMnN, we find that the Mn-induced local moment of N is negative when the Mn concentration is high ($x=1$), but changes to positive value when the Mn concentration is small. This can be understood by noticing that due to the high electronegativity of N, both the spin-up and spin-down Mn 3*d* states are higher in energy than the N 2*p* levels [Figs. 2(c) and 2(d)]. For high Mn concentration, the strong *p-d* coupling results in a high crystal field splitting, pushing the unoccupied Mn t_{2d} state to a higher energy, so that only the e_d state is mostly occupied [Fig. 2(c)]. This leads to a low-spin configuration at the Mn site ($\sim 1.4\ \mu_B$) and antiferromagnetic coupling between the Mn ions.[17] Because the spin-up Mn t_{2d} state energy is slightly lower than that of spin-down Mn t_{2d} state energy, the slightly stronger *p-d* hybridization in the spin-up channel leads to a small negative local moment on the N site. At low Mn concentration, however, the *p-d* coupling is reduced. When the crystal field splitting is smaller than the exchange splitting, Mn will have a high-spin configuration at the Mn site ($\sim 3.4\ \mu_B$), where the spin-up Mn t_{2d} state is now mostly occupied and the spin-down Mn e_d state is mostly unoccupied [Fig. 2(d)]. Because the occupied spin-up Mn t_{2d} state also contains spin-up N *p* character due to hybridization, it increases the spin-up character at the N site, switching its moment from negative to positive. The creation of holes at the nominally Mn t_{2d} state also results in a ferromagnetic coupling between the Mn ions.

Our analysis above shows that in GaMnAs, the system has a ferromagnetic ground state, which is accompanied by a negative local moment at the As site. For CdMnTe, because it has no hole at the VBM, the system has an antiferromagnetic ground state, and the local moment at the Te site is positive in the ferromagnetic phase. For GaMnN, as the system's ground state changes from antiferromagnetic to ferromagnetic, the local moment at N site also changes from negative to positive values in the ferromagnetic phase.

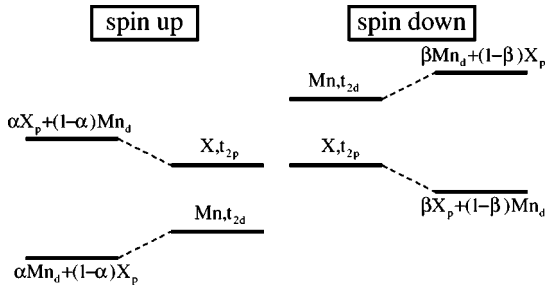

FIG. 4. Schematic plot to show the hybridization-induced mixing of the charge character of spin-up and spin-down Mn t_{2d} and anion t_{2p} levels.

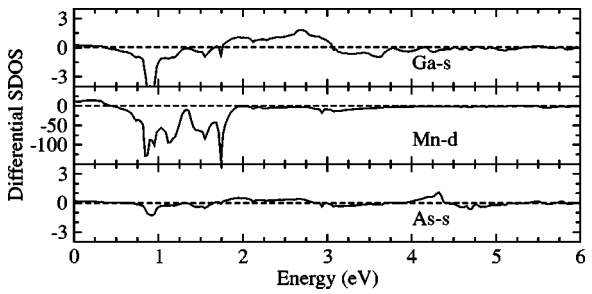

FIG. 5. Differential spin density of states for atoms in $Ga_{0.75}Mn_{0.25}As$. The zero is at the Fermi energy.

TABLE II. Core-orbital eigenvalue difference $\Delta\epsilon_c = \epsilon_c^{\downarrow} - \epsilon_c^{\uparrow}$ (in eV) for the three DMS at different concentrations. $3p_{1/2}$ eigenvalues are considered for Ga, Mn, and As; $4p_{1/2}$ is used for Cd and Te and $1s_{1/2}$ orbitals are used for N.

	$Ga_{1-x}Mn_xAs$		$Ga_{1-x}Mn_xN$		$Cd_{1-x}Mn_xTe$	
x	Atom	$\Delta\epsilon_c$	Atom	$\Delta\epsilon_c$	Atom	$\Delta\epsilon_c$
1.00	Mn	3.763	Mn	1.508	Mn	4.477
	As	−0.018	N	−0.039	Te	0.015
	Mn	3.766	Mn	3.707	Mn	4.368
0.25	Ga	0.003	Ga	0.010	Cd	0.004
	As	−0.004	N	0.018	Te	0.004

Therefore, Mn-induced local moments at the host site are strongly correlated to the magnetic coupling of Mn ions.

We have considered whether the host local moment is reflected in the differential spin DOS, as assumed in magneto-optical measurement (e.g., XMCD).[11,12] Table II lists the splitting of the core levels. We find that the sign of the spin splitting of the localized core states is strongly correlated to the local moments shown in Table I. When the moment is positive, the splitting $\Delta\epsilon_c = \epsilon_c^{\downarrow} - \epsilon_c^{\uparrow}$ is also positive. This is because the splitting of the localized state is caused mainly by the direct (potential) exchange, which is proportional to the local moment. On the other hand, we find that the correlation does not exist for the extended unoccupied conduction *s* and *p* states. For example, in Fig. 5 we show the calculated differential SDOS of the unoccupied conduction band states. We observe that although Ga in GaMnAs has a very small *positive* moment, the differential SDOS shows a large *negative* peak at a position where Mn has a large spin-down density. This is because for these extended states, the differential SDOS is mainly determined by hybridization with the spin-polarized Mn 3*d* states. Our results suggest that deducing the moment of host elements using techniques such as XMCD, which samples the extended conduction band state, requires a prior detailed knowledge of the band structure.[11] We propose that a possible alternative would be to measure the spin-polarized photoemission of the shallow core state.[22]

IV. SUMMARY

In summary, we calculate the atom and angular momentum-resolved local moments in diluted GaMnAs, GaMnN, and CdMnTe. We find that the local moments are correlated with the magnetic stability of these systems and can be explained by the occupation and hybridization of the host states with the Mn 3*d* states in both spin channels. We propose that spin-polarized photoemission measurement of the shallow core state could be used to measure the local moments of the host elements.

ACKNOWLEDGMENTS

The work at Fudan is supported by the National Science Foundation of China. X.G.G. is also supported by the Nature Science Foundation of China and Chinese Academy of Science. The work at NREL is funded by the U.S. Department of Energy, Office of Science, Basic Energy Sciences, under Contract No. DE-AC36-99GO10337 to NREL.

[1] *Diluted Magnetic Semiconductors*, edited by J. K. Furdyna and J. Kossut (Academic, Boston, 1988).
[2] H. Ohno, Science **281**, 951 (1998).
[3] T. Dietl, H. Ohno, F. Matsukura, J. Cibert, and D. Ferrand, Science **287**, 1019 (2000).
[4] D. D. Awschalom and R. K. Kawakami, Nature (London) **408**, 923 (2000).
[5] S.-H. Wei and Alex Zunger, Phys. Rev. B **35**, 2340 (1987).
[6] T. Dietl and H. Ohno, MRS Bull. **28**, 714 (2003).
[7] P. M. Krstajic, V. A. Ivanov, F. M. Peeters, V. Fleurov, and K. Kikoin, Europhys. Lett. **61**, 235 (2003); P. M. Krstajic, F. M. Peeters, V. A. Ivanov, and V. Fleurov, Phys. Rev. B **70**, 195215 (2004).
[8] K. Ando, H. Saito, V. Zayets, and M. C. Debnath, J. Phys.: Condens. Matter **16**, S5541 (2004).
[9] K. Sato, P. H. Dederics, and H. Katayama-Yoshida, Europhys. Lett. **61**, 403 (2003).
[10] B. Beschoten, P. A. Crowell, I. Malajovich, D. D. Awschalom, F. Matsukura, A. Shen, and H. Ohno, Phys. Rev. Lett. **83**, 3073 (1999).
[11] D. J. Keavney, D. Wu, J. W. Freeland, E. Johnston-Halperin, D. D. Awschalom, and J. Shi, Phys. Rev. Lett. **91**, 187203 (2003).
[12] W. L. O'Brien and B. P. Tonner, Phys. Rev. B **50**, 12 672 (1994).
[13] S.-H. Wei and H. Krakauer, Phys. Rev. Lett. **55**, 1200 (1985); D. J. Singh, *Planewaves, Pseudopotentials, and the LAPW Method* (Kluwer, Boston, 1994).
[14] J. P. Perdew and Y. Wang, Phys. Rev. B **45**, 13 244 (1992).
[15] H. J. Monkhorst and J. P. Pack, Phys. Rev. B **13**, 5188 (1976).
[16] *Semiconductors-Basic Data*, edited by O. Madelung (Springer-Verlag, New York, 1996).
[17] A. Janotti, S.-H. Wei, and L. Bellaiche, Appl. Phys. Lett. **82**, 766 (2003).
[18] Y. J. Zhao, W. T. Geng, K. T. Park, and A. J. Freeman, Phys. Rev. B **64**, 035207 (2001).

[19] E. Kulatov, H. Nakayama, H. Mariette, H. Ohta, and Y. A. Uspenskii, Phys. Rev. B **66**, 045203 (2002).
[20] S. Sanvito, P. Ordejon, and N. Hill, Phys. Rev. B **63**, 165206 (2001).
[21] H. Ohldag, V. Solinus, F. U. Hillebrecht, J. B. Goedkoop, M. Finazzi, F. Matsukura, and H. Ohno, Appl. Phys. Lett. **76**, 2928 (2000).
[22] A. Fujimori and T. Mizokawa, in *II-VI Semiconductor Compounds*, edited by M. Jain (World Scientific, Singapore, 1993), p. 103.